Journal of the European Ceramic Society 22 (2002) 2841–2848

www.elsevier.com/locate/jeurceramsoc

Effect of heat treatment of alumina granules on the compaction behavior and properties of green and sintered bodies

Nobuhiro Shinohara[a], Shigemi Katori[a], Masataro Okumiya[a], Tadashi Hotta[b], Kenji Nakahira[b], Makio Naito[b,*], Yong-Ick Cho[c], Keizo Uematsu[d]

[a]*Research Center, Asahi Glass Co., Ltd., Hazawa-cho, Kanagawa-ku, Yokohama, 221-8755, Japan*
[b]*Japan Fine Ceramics Center, 2-4-1, Mutsuno, Atsuta-ku, Nagoya 456-8587, Japan*
[c]*Engineering Research Institute Chonnam National University, 300 Yong Bong-Dong, Buk-ku, Kwang-ju, 500-757, Republic of Korea*
[d]*Department of Chemistry, Nagaoka University of Technology, 1603-1, Kamitomioka-cho, Nagaoka 940-2188, Japan*

Received 27 October 2001; received in revised form 15 March 2002; accepted 24 March 2002

Abstract

The effects of the heat treatment of Al_2O_3 granules on the fracture behavior and compressibility of the granules, as well as on the properties of the green and sintered bodies, were examined. Heat treatment contributed to increasing the strength of granules, resulting in poor deformability. However, the hard and brittle characteristics of the heat-treated granules did not hinder the promotion of uniform powder packing and the formation of a nearly cohesive compact under high compaction pressure. Although as-spray-dried granules were more deformable during compaction, they left clear interfaces between granules in the green bodies, resulting in the preservation of large pores in the samples after sintering. The high density and small pore size in green compacts formed with heat-treated granules contributed to reducing the pore-defect size in the sintered bodies, resulting in high fracture strength.

Keywords: Al_2O_3; Failure analysis; Mechanical properties; Microstructure-final; Microstructure-prefiring

1. Introduction

Granules often retain their shape in green compacts during consolidation.[1–6] Intergranular pores and flaws caused by the incomplete deformation and fracture of granules usually are large and often exert a serious influence on the properties of the final products.[7–13] Irregularly shaped granules with a dimple at the center also cause the formation of large pore defects in pressed compacts.[14] Thus, reducing the size and concentration of the pores in green bodies is crucial for the fabrication of highly reliable ceramics with high strength, because both intergranular and dimple-originated pores have a negative effect on the densification of green compacts during sintering and on the fracture-strength distribution of the resultant sintered bodies.

A recent study[15] demonstrated that the microstructure and fracture strength of granular compacted and sintered Al_2O_3 ceramics are influenced by the alteration of the dewaxing procedure. The dewaxing of mold-pressed powder compacts by heat treatment before cold-isostatic pressing effectively reduces the pore defect size in the green and sintered bodies and improves the fracture strength of the sintered bodies. The heat treatment of spray-dried granules has been reported to increase the yield pressure and cause the formation of large intergranular voids in the sintered bodies.[1] Heat-treated granules exhibited higher strength than did as-spray-dried granules in our recent study also.[15] It is interesting to clarify why heat treatment before cold-isostatic pressing contributes to reducing the size and number of pore defects in green bodies, because the consolidation of a compact during cold-isostatic pressing should be governed by the characteristics of the granules.

The objective of this paper is to clarify the effect of heat treatment of granules on their fracture strength

* Corresponding author. Tel.: +81-52-871-3500; fax: +81-52-871-3599.
E-mail address: naito@jfcc.or.jp (M. Naito).

0955-2219/02/$ - see front matter
PII: S0955-2219(02)00059-6

and compaction behavior and also on the structure and properties of the green and sintered bodies. The fracture strength of a single granule and the apparent yield pressure of the granule beds were measured. High-resolution scanning electron microscopy (SEM) was applied to examine the consolidation behavior of granules in compacts formed under different applied pressures. Direct observation techniques and mercury porosimetry also were used to examine the internal structure of the granules and of the green and sintered bodies. The different compaction behaviors between heat-treated and as-spray-dried granules are noted here, and the relevance of those behaviors to variations in the pore structure and properties of the green and sintered bodies are discussed.

2. Experimental procedure

Al_2O_3 granules were prepared by spray-drying, according to the procedure shown in previous reports.[9–11] The starting material was low-soda Al_2O_3 (AES-11E, Sumitomo Chemical Co., Ltd., Tokyo, Japan) with an average particle size of 0.4 μm and a purity of 99.8%, containing 300 ppm of MgO as a sintering agent. Poly(vinyl alcohol) and wax were added as binders, and the amount of organic components in the binders and other additives was controlled to be 0.5 mass% to the weight of the Al_2O_3 powder.

The granules then were divided into two groups, as shown in Fig. 1. One group was heat-treated at 500 °C for 5 h to remove added binders. This first group is designated A granules; the subscript "A" is also attached to the green and sintered bodies made from A granules in the following description. The other group, designated B granules, was used for testing with no treatment. The fracture behavior of a single granule was analyzed using a diametral micro-compression testing machine (Model No. PCT-200, Shimadzu Corp., Kyoto, Japan) for the granules in both groups. The fracture strength of the granules was determined from the compressive load-deformation displacement curves.[16] The compaction behavior of the granule beds was analyzed using a compression tester (Aggrobot, Hosokawa Micron Corp., Osaka, Japan).[16] For the experiment, granules were loaded into a 15 mm diameter steel die and compacted at a rate of 0.1 mm/s until the compressive stress had reached 11.1 MPa.

The sintering test was performed on cold-isostatically pressed green compacts measuring 50 mm×60 mm×10 mm. Samples were prepared by uniaxially pressing the granules at 9.8 MPa with a metal mold and cold-isostatically pressing at 176 MPa. The green densities were measured from the pore-distribution data determined by mercury porosimetry. Sintering was conducted in air

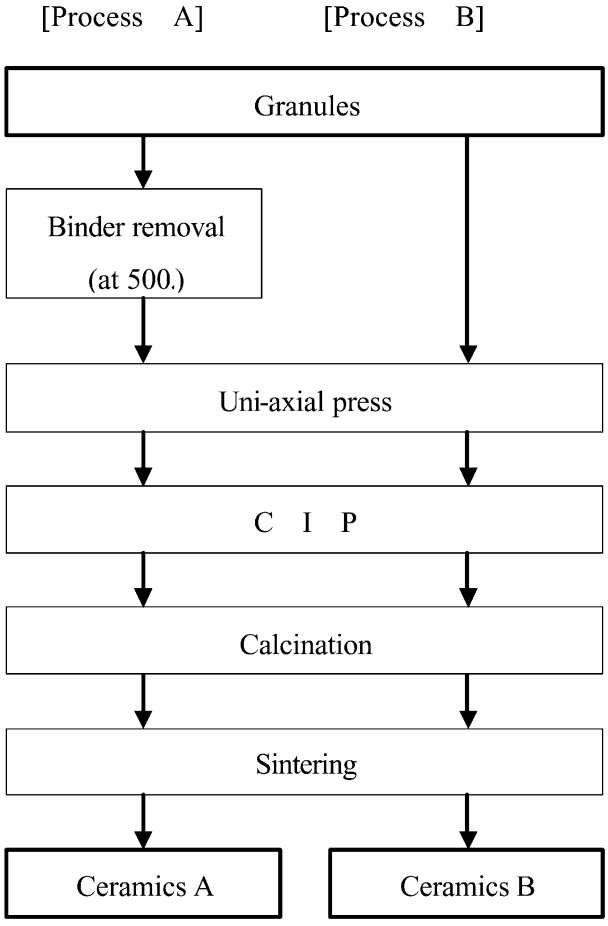

Fig. 1. Production processes of alumina ceramics.

at 1590 °C for 2 h, after calcination at 500 °C for 5 h in an electric furnace. The densities of the sintered samples were measured using the Archimedes method, with water as the immersion medium. Test samples measuring 3 mm×4 mm×40 mm were cut from the sintered samples for the measurement of fracture strength and toughness. The surface of the samples was finished with a No. 800 diamond grinding wheel. The four-point bending strength was measured for the samples according to JIS R 1601,[30] using a universal testing machine with a crosshead speed of 0.5 mm/min. The single-edged-precracked-beam method was applied to measure the fracture toughness according to JIS R 1607.[31]

Mercury porosimetry (Model No. Autopore II 9220, Micromeritics Instrument Corp., Norcross, GA) was used to determine the size and the size distribution of the pore channels in the green compacts. The internal structures of the green bodies were characterized by two methods: observation of their fracture surface by SEM and examination of their internal structure in the transmission mode, for thinned samples in an immersion liquid, according to a procedure reported

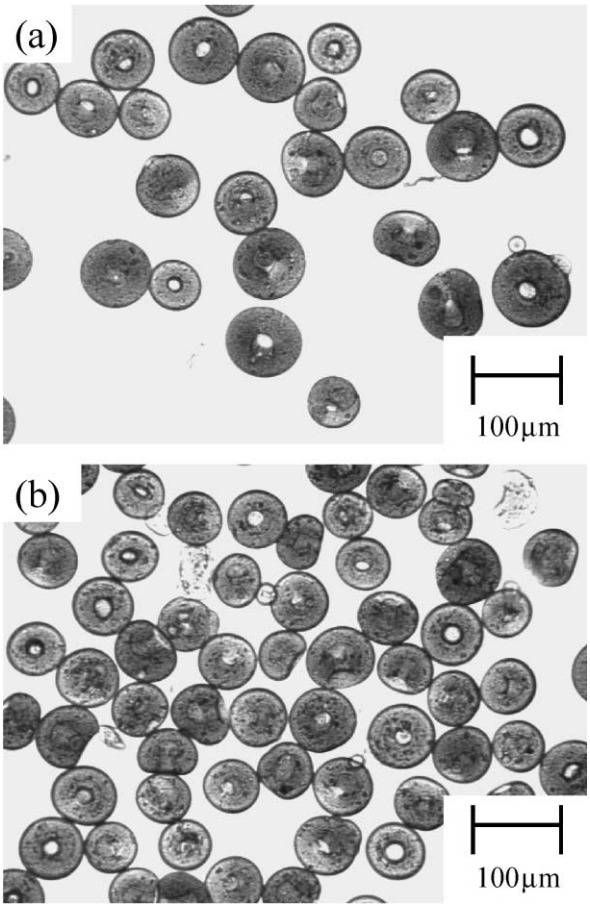

Fig. 2. Normal optical micrographs of (a) heat-treated granules A and (b) as-spray-dried granules B taken with the liquid immersion method.

elsewhere.[17–21] The internal structure of the sintered bodies also was examined in the transmission mode, for thinned samples with no immersion liquid.

3. Results

Fig. 2 shows normal optical micrographs of granules A and B, taken using the liquid-immersion method. As shown, all of the granules contained dimples. No clear difference was observed between the internal structures of the as-spray-dried and the heat-treated granules.

Fig. 3 shows the Weibull distribution curves of the diametral compression strength of granules in both groups. The maximum tensile stress was determined from the following equation, derived by Hiramatsu et al.[22] to calculate the strength of a brittle, spherically shaped sample tested in diametral compression:

$$\sigma = 2.8P_{\max}/(\pi d_G^2) \quad (1)$$

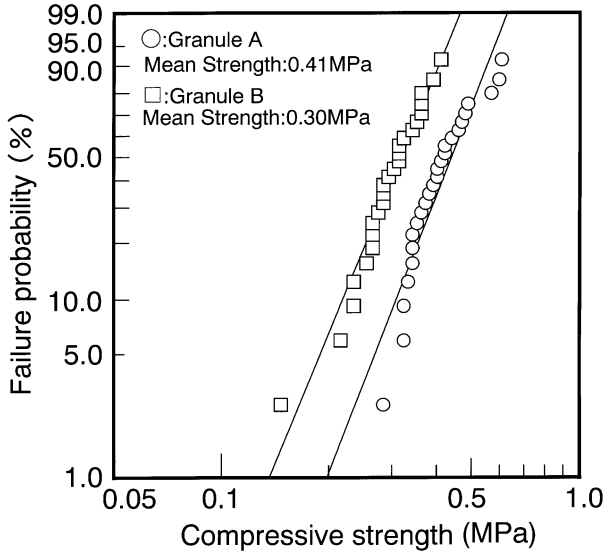

Fig. 3. Weibull distribution curves of the diametral compression strength of the granules A and B.

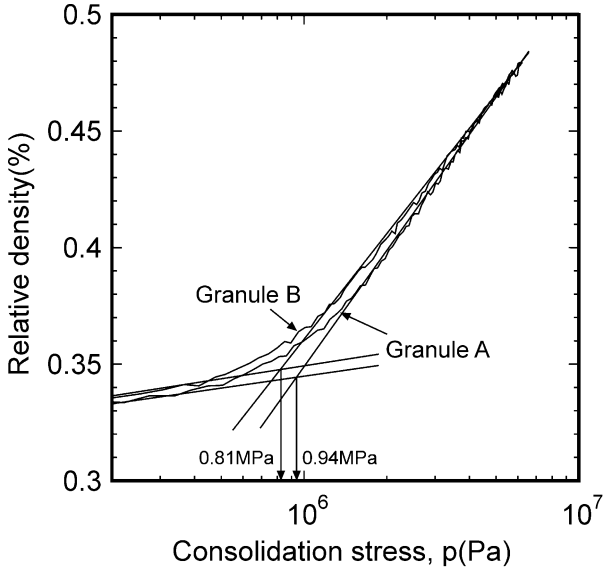

Fig. 4. Compression behavior of granule beds for granules A and B.

where σ is the maximum tensile stress (Pa), $P_{\max}$ the maximum compressive load (N), and d_G the granule diameter (m). The average strength of the heat-treated A granules (0.41 MPa) clearly was higher than that of the as-spray-dried B granules (0.30 MPa).

Fig. 4 shows the compression behavior of the granule beds. The apparent yield pressure, determined by the intersection of two straight lines fit to the low-pressure and high-pressure legs, was slightly higher for the A granules than for the B granules. Clearly, heat treatment of the granules caused an increase of the yield pressure, as expected from the results of a diametral compression

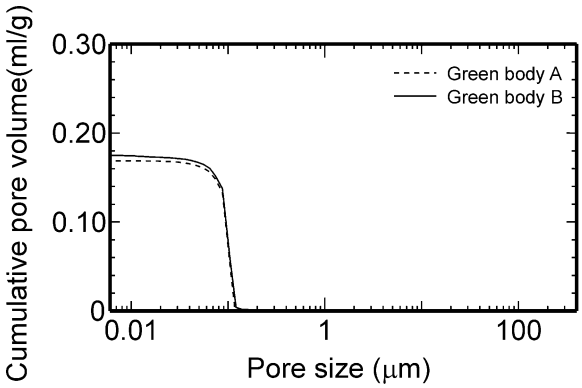

Fig. 5. Pore size distribution curves of powder compacts made from heat-treated granules A and as-spray dried granules B by cold isostatic pressing at 176 MPa.

test for a single granule. These results are consistent with those shown by Lukasiewicz and Reed,[1] who described the effect of heat treatment on the fracture behavior of Al_2O_3 granules. Fig. 4 also shows that the density of a packed bed of B granules is slightly higher than that of a packed bed of A granules at and around the yield pressure. However, the difference in the slope of these compaction curves suggests that the density would become higher for the A granules if the pressure were increased well above the yield stress, provided that the curves could be extrapolated to the high-pressure region.

Fig. 5 shows the pore-size distribution curves of powder compacts made from heat-treated and as-spray-dried granules by cold-isostatic pressing at 176 MPa. No significant difference was observed between the curves of the two compacts, although the mercury penetration volume was slightly larger for the green body B made from the as-spray-dried granules.

Figs. 6 and 7 show SEM micrographs taken on the fracture surfaces of green compacts pressed at 9.8 and 176 MPa for green body A (Fig. 6) and B (Fig. 7), respectively. A marked difference is shown in the fracture of granules for the two bodies. For the as-spray-dried B granules, traces of the granules are clearly visible in the compact pressed at a low compaction pressure, 9.8 MPa [Fig. 7(a)], although most of the granules suffered a substantial amount of plastic deformation. Only some of the granules appear to have begun to be crushed. When the pressure was increased to 176 MPa,

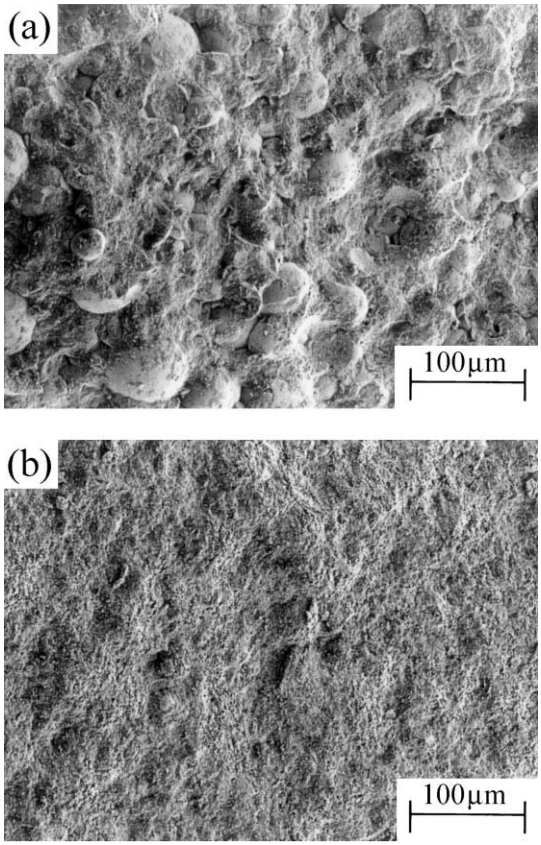

Fig. 6. SEM micrographs taken on the fracture surface of green compacts A (made from heat-treated granules A) by pressing at (a) 9.8 MPa and (b) 176 MPa.

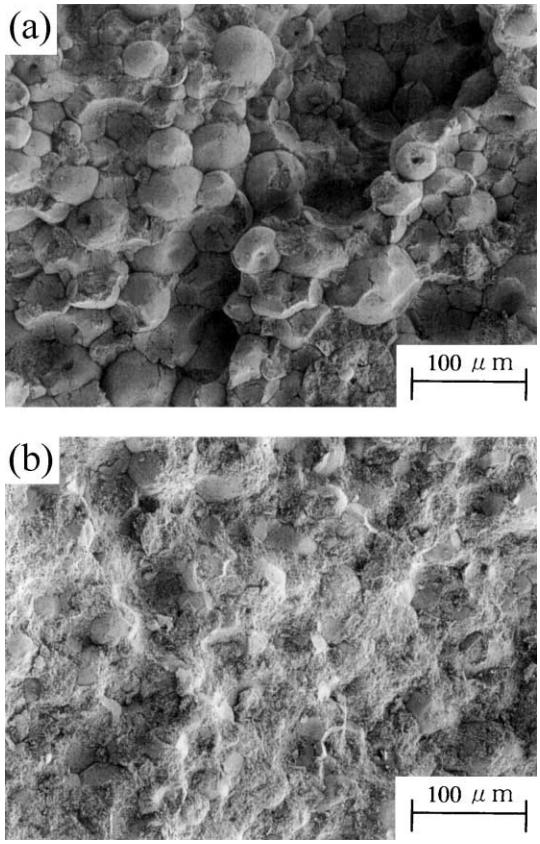

Fig. 7. SEM micrographs taken on the fracture surface of green compacts B (made from as-spray-dried granules B) by pressing at (a) 9.8 MPa and (b) 176 MPa.

many granules fractured, as shown in [Fig. 7(b)]. However, the compact was still composed of unfractured granules, with powder particles filling the void spaces between granules. For the heat-treated A granules, on the other hand, many granules were already fractured, even at a low compaction pressure [Fig. 6(a)]. The noticeable deformation found in almost all of the B granules is hardly observable on the surface of the unfractured, persistent A granules. After cold-isostatic pressing at 176 MPa, the A granules appear to be fully fractured, to form a nearly cohesive compact [Fig. 6(b)], showing the promotion of uniform powder packing for A granules during compaction.

Fig. 8 shows normal optical micrographs taken in the transmission mode, by the liquid-immersion method, for green compacts A and B cold-isostatically pressed at 176 MPa. The traces of granules and the void spaces in and between the granules are visible in both compacts. These void spaces were not detectable by mercury porosimetry because of their low concentration.[5] As shown, the interfaces of the trace granules and the large number (volume) of void spaces were more evident in green body B. Because the boundaries and void spaces are formed by the incomplete adhesion of powder particles in and between granules, the results again show improved powder packing in green body A.

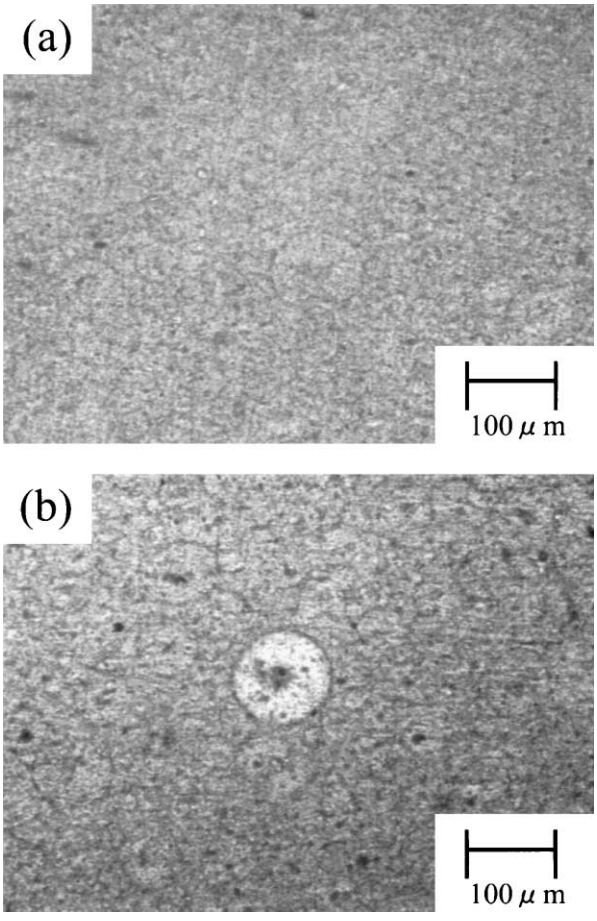

Fig. 8. Normal optical micrographs taken in the transmission mode with the liquid immersion method for the (a) green body A and (b) green body B which were cold isostatically pressed at 176 MPa.

Fig. 9 shows the Weibull distribution curves of fracture strength measured for sintered samples in both groups. The variations shown in fracture strength indicate the marked influence of heat treatment of the granules on the properties of the sintered bodies. The fracture strength of the sintered body A (averaging 489 MPa) was clearly higher than that of the sintered body B (411 MPa). The Weibull modulus was high for both samples, suggesting that the fracture origins were uniformly large.

Fig. 10 shows photomicrographs taken in the transmission mode, on thinned samples, for both sintered bodies A and B. Many large pores are shown in and between the traces of granules for both samples, even after sintering, although the size and number of the pores are clearly small in the sintered body A made from the heat-treated granules.

The properties of the green and sintered bodies are summarized in Table 1. The densities of the green compacts were calculated from the pore volume determined by mercury porosimetry for calcined samples at 500 °C. The density of the powder compacts pressed at a pressure of 9.8 MPa was higher for the compacts from granules A (2.08×10^3 kg/m^3) than for those from granules B (2.02×10^3 kg/m^3), as expected from the extrapolation of the compaction curves, shown in Fig. 4. The difference in green density between the two samples decreased after cold-isostatic pressing at 176 MPa. However, the density was still slightly higher for green body A. The sintered bulk densities were nearly the same for both samples.

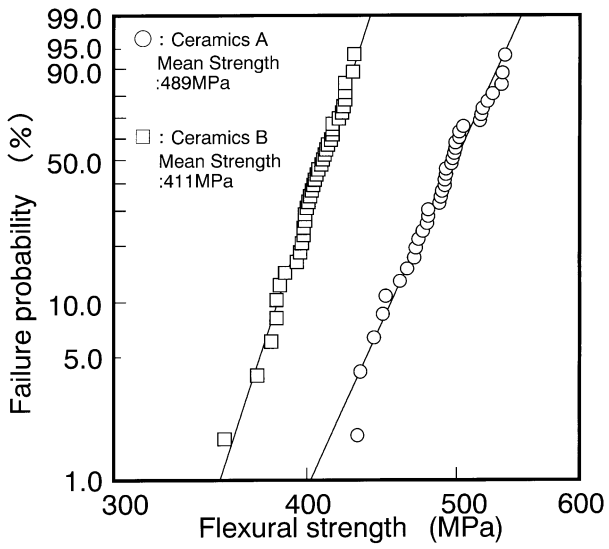

Fig. 9. Weibull distribution curves of fracture strength measured for sintered specimens A and B.

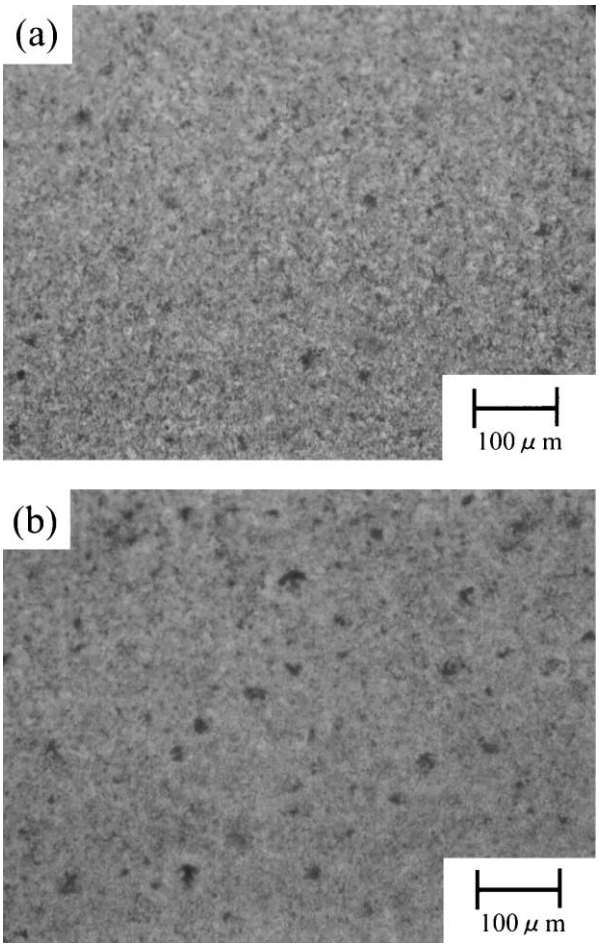

Fig. 10. Photomicrographs taken in the transmission mode on thinned specimens for the (a) sintered body A and (b) sintered body B.

Table 1
Properties of green and sintered bodies made from heat-treated granules A and as-spray-dried granules B

	Density of green body (kg/m^3)		Density of sintered body (kg/m^3)	Flexural strength (MPa)	Fracture toughness (MPa m$^{1/2}$)
	9.8 MPa	176 MPa			
Process A	2.08×10^3	2.35×10^3	3.93×10^3	489	4.9
Process B	2.02×10^3	2.33×10^3	3.92×10^3	411	4.7

4. Discussion

Variation of the strength of Al_2O_3 ceramics fabricated through the granular compaction route is governed by the pore-size distribution in the sintered bodies, especially that of large pores, measuring nearly 100 μm.[10–13] Potential flaws are first introduced into the green compacts during forming, then persist or develop to strength-limiting large pore defects during the subsequent densification process.[23–25] For processing using powder granules, major potential flaws in the green compacts are the residual pores or cracks in and between the trace granules, caused by the incomplete deformation and fracture of the granules.

Incomplete deformation and fracture of the granules during compaction are also responsible for the density distribution in the pressed compacts, because of non-uniform powder packing between the packed layer of powder particles near the surface of the trace granules and internal less-dense regions in which pores or cracks exist.[25] Nonuniform powder packing results in differential densification between the highly packed and the less-dense regions with sintering, causing the development of void spaces in the less-dense regions to form large pore defects.[24,25] Introduction of these heterogeneities into the green compacts is related to the characteristics of the granules, as well as to the compaction behavior, so that soft and deformable granules are favored to promote uniform powder packing with better joining at their boundaries and to achieve high green density with small pore size.[2–4, 26–29]

The present results indicate that even hard and less-deformable granules can result in enhanced powder packing during compaction and in improved fracture strength of the sintered body. Figs. 3 and 4 show that the heat-treated A granules had higher strength for a single granule and higher yield pressure for the granule bed than did the as-spray-dried B granules. Furthermore, as demonstrated in Figs. 6 and 7, the B granules had more deformable characteristics in the pressed compacts under applied pressure.

According to results from past studies, the B granules should have induced more efficient powder packing for densification. At and around the apparent yield pressure, defined to be the critical stress at which granule rearrangement is essentially complete and granule deformation and/or fracture begins,[1–4, 29] the B granules exactly provided higher packing density, as shown in Fig. 4. However, when the applied pressure was increased, the density of the pressed compacts became higher for those made from the A granules than for those made from the B granules, as expected from the extrapolation of the compaction curves.

The results for the measurement of fracture strength (Fig. 9) and for observation of the internal structures (Fig. 10) of the sintered bodies also strongly suggest that A granules promoted efficient powder packing during compaction. A comparison of Figs. 8 and 10 indicates that the large pore defects in the sintered bodies developed during sintering, from the pores or void spaces distributed in the green compacts. The smaller size and number of large pores in the sintered body A clearly show that heat treatment of the granules contributed to reducing the size and population of potential flaws in green body A.

The difference in fracture behavior between the as-spray-dried and the dewaxed granules is the key to explaining the present compaction behavior. As presented in Fig. 7, the as-spray-dried B granules only suffered plastic deformation in the compact pressed at a pressure 9.8 MPa, and, as a result, the traces of granules were preserved. On the other hand, as shown in Fig. 6, the heat-treated A granules began to be crushed, without noticeable deformation, at 9.8 MPa. This result suggests that the A granules fractured in the brittle mode. Because of this hard and brittle characteristic, the A granules seemed only to slide across each other for rearrangement, with a smaller increase in density than in the B granules, which were accompanied by deformation in the low-pressure range near the apparent yield pressure.

As the applied compaction pressure was increased, granules with relatively low breakage value began to be crushed, so that the primary powder particles filled the void spaces between the unfractured granules. Densification of the compacts of the A granules proceeded by the rearrangement of both granules and primary particles, to form a denser packing configuration than that of the B granules, for which plastic deformation of the granules was a dominant mechanism during compaction. At a high pressure, 176 MPa, for cold-isostatic pressing, Figs. 6 and 7 suggest that the A granules appear to be fully fractured, to form a nearly cohesive compact, whereas that the B granules form a compact composed of unfractured granules, with powder particles between the granules.

However, the normal optical micrographs taken in the transmission mode indicate that, even for the A granules, the traces of granules and the void spaces in and between the granules were preserved in the green body as shown in Fig. 8. One interpretation is that, in compacts made with the A granules, the fracture occurs through the debris between largely intact granules as shown in Fig. 6.This is entirely consistent with what has been seen elsewhere for brittle granules.[32] That explains many brittle granules survive intact because they are protected by the surrounding debris as shown in Fig. 8. However, the interfaces between the trace granules were less clear, and the size and number of large pores that developed to strength-limiting defects during densification with sintering were smaller for the green body A.

Thus, the consolidation behavior of the granules cannot be estimated by examining the fracture of a single granule or the compression behavior of the granule beds alone. It is important to examine in detail configurational change of the granules and pores in the products at each processing stage, along with observation of the internal structure by such techniques as SEM and direct observation, in order to achieve improved microstructure and properties for the final products.

5. Conclusions

The heat treatment of Al_2O_3 granules effectively reduced the size and population of potential flaws in the green bodies during compaction under a high applied pressure. Heat treatment resulted in high strength for Al_2O_3 ceramics after sintering. The hard and brittle characteristics of the heat-treated granules contributed to achieving a uniform packing structure in the green body, because the spaces between granules were efficiently filled with primary powder particles caused by fracture of the granules. On the other hand, the as-spray-dried granules preserved more clear interfaces between granules and internal pores in the green compacts, resulting in the development of large pores, and, thus, a decrease in fracture strength for the sintered body.

Acknowledgements

This work was supported by the New Energy and Industrial Technology Development Organization (NEDO) as a part of the International Joint Research Program (NEDO GRANT). This work was also supported by Korea Research Foundation Grant (KRF-Y00316).

References

1. Lukasiewicz, S. J. and Reed, J. S., Character and compaction response of spray-dried agglomerates. *Am. Ceram. Soc. Bull.*, 1978, **57**, 798–801.
2. Youshaw, R. A. and Halloran, J. M., Compaction of spray-dried powders. *Am. Ceram. Soc. Bull.*, 1992, **61**, 227–230.
3. Dimilia, R. A. and Reed, J. S., Dependence of compaction on the glass transition temperature of the binder phase. *Am. Ceram. Soc. Bull.*, 1983, **62**, 484–488.
4. Frey, R. G. and Halloran, J. W., Compaction behavior of spray-dried alumina. *J. Am. Ceram. Soc.*, 1984, **67**, 199–203.
5. Uematsu, K., Miyashita, M., Kim, J.-Y., Kato, Z. and Uchida, N., Effect of forming pressure on the internal structure of alumina green bodies examined with immersion liquid technique. *J. Am. Ceram. Soc.*, 1991, **74**, 2170–2174.
6. Takahashi, H., Shinohara, N., Okumiya, M., Uematsu, K., Iwamoto, Y., Tsubaki, J. and Kamiya, H., Influence of slurry flocculation on the character and compaction of spray-dried silicon nitride granules. *J. Am. Ceram. Soc.*, 1995, **78**, 903–908.
7. Takahashi, H., Shinohara, N., Uematsu, K. and Tsubaki, J., Influence of granule character and compaction on the mechanical properties of sintered silicon nitride. *J. Am. Ceram. Soc.*, 1996, **79**, 843–848.
8. Iwamoto, Y., Nomura, H., Sugiura, I., Tsubaki, J., Takahashi, H., Ishikawa, K., Shinohara, N., Okumiya, M., Yamada, T., Kamiya, H. and Uematsu, K., Microstructure evolution and mechanical strength of silicon nitride ceramics. *J. Mat. Res.*, 1994, **9**, 1208–1213.
9. Shinohara, N., Okumiya, M., Hotta, T., Nakahira, K., Naito, M. and Uematsu, K., Effect of seasons on density, strength of alumina. *Am. Ceram. Soc. Bull.*, 1999, **78**, 81–84.

10. Shinohara, N., Okumiya, M., Hotta, T., Nakahira, K., Naito, M. and Uematsu, K., Seasonal variation of microstructure and sintered strength of dry-pressed alumina. *J. Am. Ceram. Soc.*, 1999, **82**, 3441–3446.
11. Shinohara, N., Okumiya, M., Hotta, T., Nakahira, K., Naito, M., Uematsu, K. and Formation mechanisms of processing defects, their relevance to the strength in alumina ceramics made by powder compaction process, *J. Mater. Sci.*, 1999, **34**, 4271–4277.
12. Hotta, T., Nakahira, K., Naito, M., Shinohara, N., Okumiya, M. and Uematsu, K., Origin of strength change in ceramics associated with the alteration of spray dryer. *J. Mater. Res.*, 1999, **14**, 2974–2979.
13. Zhang, Y., Inoue, M., Uchida, N. and Uematsu, K., Characterization of processing pores and their relevance to the strength in alumina ceramics. *J. Mater. Res.*, 1999, **14**, 3370–3374.
14. Walker, W. J. Jr., Reed, J. S. and Verma, S. K., Influence of granule character on strength and weibull modulus of sintered alumina. *J. Am. Ceram. Soc.*, 1999, **82**, 50–56.
15. Shinohara, N., Okumiya, M., Hotta, T., Nakahira, K., Naito, M. and Uematsu, K., Variation of the microstructure and fracture strength of cold isostatically pressed alumina ceramics with the alteration of dewaxing procedures. *J. Eur. Ceram. Soc.*, 2000, **20**, 843–849.
16. Naito, M., Nakahira, K., Hotta, T., Ito, A., Yokoyama, T. and Kamiya, H., Microscopic analysis on the consolidation process of granule beds. *Powder Technology*, 1998, **95**, 214–219.
17. Uematsu, K., Kim, J.-Y., Kato, Z., Uchida, N. and Saito, K., Direct observation method for internal structure of ceramic green body-alumina green body as an example. *J. Ceram. Soc. Japan*, 1990, **98**, 515–516.
18. Uematsu, K., Kim, J.-Y., Miyashita, M., Uchida, N. and Saito, K., Direct observation of internal structure in spray-dried alumina granules. *J. Am. Ceram. Soc.*, 1990, **73**, 2555–2557.
19. Uematsu, K., Tanaka, T., Zhang, Y. and Uchida, N., Liquid immersion-polarized light microscopy as a powerful tool in the research of ceramic processing. *J. Ceram. Soc. Japan.*, 1993, **101**, 1400–1403.
20. Uematsu, K., Immersion microscopy for detailed characterization of defects in ceramic powders and green bodies. *Powder Technology*, 1996, **88**, 291–298.
21. Uematsu, K., Miyashita, M., Kim, J.-Y. and Uchida, N., Direct study of the behavior of flaw-forming defect in sintering. *J. Am. Ceram. Soc.*, 1992, **75**, 1016–1018.
22. Hiramatsu, Y., Oka, Y. and Kiyama, H., Determination of the tensile strength of rock by a compression test of an irregular test piece. *J. Min. Eng. Jpn.*, 1965, **81**, 1024–1030.
23. Lange, F. F., Powder processing science and technology for increased reliability. *J. Am. Ceram. Soc.*, 1989, **72**, 3–15.
24. Lange, F. F., Sinterability of agglomerated powders. *J. Am. Ceram. Soc.*, 1984, **67**, 83–89.
25. Shinohara, N., Okumiya, M., Hotta, T., Nakahira, K., Naito, M. and Uematsu, K., Morphological changes in process-related large pores of granular compacted and sintered alumina. *J. Am. Ceram. Soc.*, 2000, **83**, 1633–1640.
26. Nies, C. W. and Messing, G. L., Effect of glass-transition temperature of polyethylene glycol-plasticized polyvinyl alcohol on granule compaction. *J. Am. Ceram. Soc.*, 1984, **67**, 301–304.
27. Tanaka, H., Fukai, S., Uchida, N. and Uematsu, K., Effect of moisture on the structure and fracture strength of ceramic green bodies. *J. Am. Ceram. Soc.*, 1994, **77**, 3077–3080.
28. Zheng, J. and Reed, J. S., Particle and granule parameters affecting compaction efficiency in dry pressing. *J. Am. Ceram. Soc.*, 1988, **71**, C456–C458.
29. Messing, G. L., Markoff, C. J. and McCoy, L. G., Characterization of ceramic powder compaction. *Am. Ceram. Soc. Bull.*, 982, **61**, 857–860.
30. *Japanese Industrial Standard, R 1601. Testing Method for Flexural Strength (Modulus of Rupture) of Fine Ceramics*. Japanese Standards Association, Tokyo, Japan, 1995.
31. *Japanese Industrial Standard, R 1607. Testing Methods for Fracture Toughness of Fine Ceramics*. Japanese Standards Association, Tokyo, Japan, 1995.
32. Steacy, S. J. and Sammis, C. G., An automaton for fracture patterns of fragmentaion. *Nature*, 1991, **353**, 250–252.